Age-Related Networks of Regional Covariance in MRI Gray Matter: Reproducible Multivariate Patterns in Healthy Aging

Kaitlin L. Bergfield, Krista D. Hanson, Kewei Chen, Stefan J. Teipel, Harald Hampel, Stanley I. Rapoport, James R. Moeller, Gene E. Alexander

PII: S1053-8119(09)01030-1
DOI: doi:10.1016/j.neuroimage.2009.09.051
Reference: YNIMG 6600

To appear in: *NeuroImage*

Received date: 29 May 2009
Revised date: 5 September 2009
Accepted date: 22 September 2009

Please cite this article as: Bergfield, Kaitlin L., Hanson, Krista D., Chen, Kewei, Teipel, Stefan J., Hampel, Harald, Rapoport, Stanley I., Moeller, James R., Alexander, Gene E., Age-Related Networks of Regional Covariance in MRI Gray Matter: Reproducible Multivariate Patterns in Healthy Aging, *NeuroImage* (2009), doi:10.1016/j.neuroimage.2009.09.051

Age-Related Networks of Regional Covariance in MRI Gray Matter: Reproducible Multivariate Patterns in Healthy Aging

Kaitlin L. Bergfield[a,b,j], Krista D. Hanson[b,c,j], Kewei Chen[d,j], Stefan J. Teipel[e], Harald Hampel[f,g], Stanley I. Rapoport[h], James R. Moeller[i], Gene E. Alexander[a,b,c,j,*]

[a]Neuroscience Graduate Interdisciplinary Program, University of Arizona, Tucson, AZ 85721, USA

[b]Evelyn F. McKnight Brain Institute, University of Arizona, Tucson, AZ 85721, USA

[c]Department of Psychology, University of Arizona, Tucson, AZ 85721, USA

[d]Banner Alzheimer's Institute and Banner Samaritan PET Center, Banner Good Samaritan Medical Center, Phoenix, AZ 85006, USA

[e]Department of Psychiatry, University of Rostock, Rostock, Germany

[f]Discipline of Psychiatry, School of Medicine and Trinity College Institute of Neuroscience, Laboratory of Neuroimaging and Biomarker Research, The Adelaide and Meath Hospital incorporating the National Children's Hospital, Trinity College, University of Dublin, Ireland

[g]Department of Psychiatry, Alzheimer's Memorial Center, Ludwig Maximilian University, Munich, Germany

[h]Brain Physiology and Metabolism Section, National Institute on Aging, National Institutes of Health, Bethesda, MD 20892, USA

[i]Department of Psychiatry, College of Physicians and Surgeons, Columbia University, New York, NY 10032, USA

[j]Arizona Alzheimer's Consortium, Phoenix, AZ 85006, USA

*Corresponding Author: Gene E. Alexander, Ph.D., Department of Psychology, University of Arizona, Tucson, AZ 85721; Phone: (520) 626-1704; Fax: (520) 621-9306; E-mail: gene.alexander@arizona.edu

Abstract

Healthy aging is associated with brain volume reductions that involve the frontal cortex, but also affect other brain regions. We sought to identify an age-related network pattern of MRI gray matter using a multivariate statistical model of regional covariance, the Scaled Subprofile Model (SSM) with voxel based morphometry (VBM) in 29 healthy adults, 23-84 years of age (Group 1). In addition, we evaluated the reproducibility of the age-related gray matter pattern derived from a prior SSM VBM study of 26 healthy adults, 22-77 years of age (Group 2; Alexander et al., 2006) in relation to the current sample and tested the ability of the network analysis to extract an age-related pattern from both cohorts combined. The SSM VBM analysis of Group 1 identified a regional pattern of gray matter atrophy associated with healthy aging (R^2=0.64, p<0.000001) that included extensive reductions in bilateral dorsolateral and medial frontal, anterior cingulate, insula/perisylvian, precuneus, parietotemporal, and caudate regions with areas of relative preservation in bilateral cerebellum, thalamus, putamen, mid cingulate, and temporal pole regions. The age-related SSM VBM gray matter pattern, previously reported for Group 2, was highly expressed in Group 1 (R^2=0.52, p<0.00002). SSM analysis of the combined cohorts extracted a common age-related pattern of gray matter showing reductions involving bilateral medial frontal, insula/perisylvian, anterior cingulate and, to a lesser extent, bilateral dorsolateral prefrontal, lateral temporal, parietal, and caudate brain regions with relative preservation in bilateral cerebellum, temporal pole, and right thalamic regions. The results suggest that healthy aging is associated with a regionally distributed pattern of gray matter atrophy that has reproducible regional features. Whereas the network patterns of atrophy included

parietal, temporal, and subcortical regions, involvement of the frontal brain regions showed the most consistently extensive and reliable reductions across samples. Network analysis with SSM VBM can help detect reproducible age-related MRI patterns, assisting efforts in the study of healthy and pathological aging.

Introduction

It is well established that healthy aging is associated with declines in frontal lobe-mediated cognitive functions (West, 1996; Albert, 1997; Grady and Craik, 2000; Rypma et al., 2001; Buckner, 2004; Van Petten et al., 2004). Volumetric methods with magnetic resonance imaging (MRI) have shown age-related reductions in frontal regions, but have also found reductions in other brain areas, including in temporal, parietal, subcortical, cerebellar, and white matter regions (Raz et al., 1998; Good et al., 2001; Jernigan et al., 2001; Tisserand et al., 2002; Tisserand and Jolles, 2003). Most volumetric MRI studies of healthy aging to date have used univariate, manually-traced regions of interest (ROI) of anatomically defined brain structures or voxel-based regional volume maps to characterize age effects. While such univariate approaches allow for comparisons of local regional brain volume, multivariate analysis methods test for covariance patterns of regional differences in brain volume, providing a complement to univariate methods for detecting and tracking the regionally distributed effects of aging and disease.

The Scaled Subprofile Model (SSM; Moeller et al., 1987) is one form of multivariate analysis that has been applied to numerous functional (Alexander and Moeller, 1994; Alexander et al., 1999; Eidelberg et al., 1995a, b; Moeller et al., 1996; Eidelberg, 1998; Habeck et al., 2003; 2004; Stern et al., 2005; Smith et al., 2006) and more recently structural neuroimaging studies (Alexander et al., 2006; 2008; Brickman et al., 2007; 2008). As a modified form of principal component analysis (PCA), the SSM can directly test for network patterns in neuroimaging data that reflect the regionally

distributed effects of aging or disease on the brain and their relation to measures of cognition and behavior, peripheral biomarkers, or genetic risk factors.

In a previous study, we identified a multivariate network pattern of MRI gray matter associated with healthy aging using statistical parametric mapping (SPM2; Wellcome Department of Imaging Neuroscience, London, UK) voxel-based morphometry (VBM; Ashburner and Friston, 2000; Ashburner et al., 2003) combined with the SSM. In this latter study, older age was associated with greater gray matter volume reductions in bilateral frontal, temporal, thalamic, and right cerebellar regions, with relative preservation in bilateral middle and superior temporal gyri in a group of 26 healthy adults with a continuous age range extending from 22 to 77 years (Alexander et al., 2006). These findings were generally consistent with subsequent studies by Brickman et al. (2007; 2008) using SSM VBM with SPM99 to identify an age-related pattern of gray matter defined by distinguishing between two dichotomous young and old age groups that did not include middle-aged adults and by prospectively applying the age-group pattern to independent groups of similarly young and old healthy adults.

In the current study, we sought to identify an age-related multivariate network pattern of MRI gray matter using SPM5 VBM with SSM and bootstrap re-sampling in 29 neurologically healthy adults, over a continuous adult age range from 23-84 years of age. Further, we tested the reproducibility of the results from our previous MRI study of healthy aging (Alexander et al., 2006) by 1) prospectively applying the observed network pattern from the prior study to the MRI scans obtained in the current independent sample of healthy adults and 2) re-analyzing the MRI scans from our previous report using the same SPM5 post-processing and bootstrap procedures

applied in the current sample of healthy adults. Since the MRI scans for the two samples were acquired using different scan sequence parameters, we subsequently tested the ability of our network analysis method to extract an age-related pattern from both samples combined to evaluate the potential of this multivariate technique for detecting a reliable and robust age-related network pattern despite differences between cohorts in MRI sequence parameters. Finally, we evaluated the extent to which our network patterns of MRI VBM gray matter reductions in healthy aging could be explained by subject differences in an increased genetic risk for Alzheimer's dementia related to the presence of the apolipoprotein E (APOE) ε4 allele, a common susceptibility gene for late onset Alzheimer's disease (AD; Saunders et al., 1993; Reiman et al., 2001). We hypothesized that older age would be associated with a widely distributed regional network pattern of gray matter atrophy showing reductions preferentially involving frontal and selective temporal brain regions. Further, we expected that, despite the heterogeneity associated with individual differences in brain anatomy, technical differences in MRI acquisition across samples, and the APOE-associated genetic risk for dementia, our healthy aging-related MRI gray matter patterns would have common regional network features that are shared across our healthy adult cohorts with an age range extending from young to elderly adulthood.

Methods

Participants

Healthy volunteers were recruited by newspaper advertisement. Participants were grouped into three cohorts for analyses: a cohort of 29 subjects (Group 1), an

independent cohort of 26 participants (Group 2) from a previous report (Alexander et al., 2006), and a combined group from the two cohorts producing a total of 55 subjects (Combined Group). Participant demographics for the three cohorts are shown in **Table 1**. Participants in Group 1 were 23 to 84 years of age and included 11 men and 18 women. Demographics of participants in Group 2 have been described previously (Alexander et al., 2006) and included subjects with ages ranging from 22 to 77 years with 15 men and 11 women. Participants in the Combined Group were 22 to 84 years of age, including 26 men and 29 women. There was no significant difference in age between the gender groups with any of the three cohorts ($p \geq 0.21$) and there was no significant gender by cohort interaction ($p = 0.76$) for age across Groups 1 and 2.

Participants underwent an extensive medical screen to exclude any history of illness or injury that could affect brain structure or function. The screening procedures have been described in detail (Alexander et al., 1997). Briefly, these procedures included a review of medical history, neurological and physical exams, blood tests, electrocardiogram, electroencephalogram, brain MRI, neuropsychological assessment, and clinical scales. The participants were selected from a cohort of healthy adults evaluated as part of a study of aging and dementia in the Intramural Research Program at the National Institute on Aging where test results for all participants were individually reviewed and discussed to consensus at a diagnostic group conference attended by neurologists, psychiatrists, and neuropsychologists specializing in aging and dementia. All participants included in this study were medically healthy with no evidence of cognitive impairment or complaints, had Mini-Mental State Examination (MMSE; Folstein et al., 1975) scores ≥ 28, and had good-quality MRI scans. The data were part

of a National Institute on Aging Institutional Review Board approved protocol, and each participant provided informed written consent to participate.

Apolipoprotein E (APOE) alleles were determined from genomic DNA obtained from blood samples using a polymerase chain reaction (PCR) method which has been previously described in detail (Saunders et al., 1993). Briefly, genotyping was performed with DNA amplification by PCR using APOE primers and the HhaI restriction isotyping enzyme. Amplified DNA was digested by HhaI, resolved on a polyacrylamide gel, and autoradiographed for allele detection. Each autoradiograph was visualized by two independent observers who were blind to subject age and cognitive function. The Combined Group of 55 subjects consisted of 19 carriers of the APOE ε4 allele (one ε4/ ε4, 17 ε3/ε4 and one ε2/ ε4) and 36 ε4 non-carriers (30 ε3/ε3, five ε2/ε3, and one ε2/ ε2). There were no significant age ($p = 0.66$) or gender ($p = 0.61$) differences between APOE ε4 carriers and non-carriers. APOE ε4 carrier distributions for the three cohorts are shown in **Table 1**. Although the frequency of APOE ε4 carriers in this sample is 34.5%, about 10% percent higher than general population estimates, the subjects were not pre-selected on the basis of genetic risk or family history of dementia and were self-referred normal volunteers without memory complaints.

Image acquisition

In Group 1, volumetric T1-weighted SPGR MRI scans were acquired for each participant on a 1.5T scanner (GE Signa II, Milwaukee, WI, USA) with 124 contiguous sagittal 1.5 mm thick slices and 0.94 by 0.94 in plane resolution (repetition time = 14.3 msec, echo time = 5.4 msec, field of view = 24). Image acquisition parameters for

Group 2 have been described previously (Alexander et al., 2006). These scans were also obtained as volumetric T1-weighted SPGR MRI scans on the same 1.5 T GE Signa II system, but were acquired with 124 contiguous coronal 2 mm thick slices and a 0.94 by 0.94 in plane resolution (repetition time = 24 msec, echo time = 5 msec, field of view = 24).

Image processing

The MRI scans were processed using Statistical Parametric Mapping (SPM5, Wellcome Department of Imaging Neuroscience, London, UK) with VBM (Ashburner and Friston, 2000; Good et al., 2001). Briefly, for each group customized sample-specific tissue segmentation priors were created using all scans from that cohort, with the tissue priors applied for use in the iterative spatial normalization and tissue segmentation procedure. Each gray matter map was multiplied by the Jacobian determinant and smoothed using a 10-mm Gaussian kernel to produce smoothed maps of gray matter volume. An estimate of total intracranial volume (eTIV) was computed for each scan by combining the gray, white, and cerebrospinal fluid segments obtained from the SPM VBM processing.

Image Analysis

After SPM5 VBM processing, SSM analysis was performed for the voxel-based gray matter volume images using MATLAB (Math Works, Natick, Massachusetts, USA). The assumptions and procedures of the SSM have been previously described in detail (Moeller et al., 1987; Alexander and Moeller, 1994). Briefly, a PCA is performed on the

natural log transformed neuroimage data, after the means across regions and subjects are subtracted at each voxel. These procedures produce a set of regional network covariance patterns and corresponding subject scores that reflect the degree to which each subject expresses the identified network patterns. We performed SSM on VBM gray matter images to identify patterns of gray matter volume associated with age in our healthy samples. Multiple regression analysis was used to identify the best set of SSM component patterns predicting age. We first tested the significance of the regression model predicting age using the first 10 patterns of the SSM and subsequently identified the subset of those 10 patterns with significant coefficients providing the best pattern estimate of age in each sample. Additional regression analyses were used to test the effect of gender and APOE ε4 carrier status on the identified age-related network. The eTIV was subsequently used as an additional covariate to test for possible effects of individual differences in total brain intracranial size.

A bootstrap re-sampling procedure (Efron and Tibshirani, 1994) was applied with 500 iterations to the SSM analysis (Alexander et al., 2008) providing reliability estimates at each voxel for the observed pattern weights associated with age for the Group 1, Group 2, and Combined Group analyses. The bootstrap method was used to calculate confidence intervals for the voxel weights of the pattern associated with the subject score prediction of age. SSM and subject score regression analyses were performed at each iteration of the bootstrap. The set of SSM components that are used to predict age and compute the associated pattern was the smallest set whose subject scores accounted for 80% of the variance of the voxel-by-subject interactions in the MRI data set. This approach tends to conservatively allow the major sources of variance in the

MRI data to influence the computation of the reliability estimates for all voxels included in the SSM analysis.

The SPM Montreal Neurological Institute (MNI) coordinates for the local minima and maxima values from the bootstrapped SSM pattern weights were selected with Z-values ≥ +2 and ≤ -2 and were converted to coordinates from the Talairach and Tournoux (1988) brain atlas (http://www.mrc-cbu.cam.ac.uk/Imaging/Common/mnispace.html) to identify the full extent of brain regions robustly contributing to the SSM age-related patterns.

The SSM VBM gray matter pattern weights associated with healthy aging derived from our previous study (Alexander et al., 2006) were prospectively applied to the MRI scans from Group 1 to directly test the expression of the prior age-related pattern in the current independent sample. This procedure has been described previously (Eidelberg et al., 1995; Habeck et al., 2005), in which the pattern weights obtained from an image analysis can be applied to a new set of image data collected from independent samples or from repeated measurements in the same subjects. Briefly, the dot product of the gray matter map for each subject with the previously identified regional network pattern map is performed. In this case, the resulting scalar subject scores represent the degree to which each subject in the new sample manifests the previously derived pattern of gray matter volume.

Results

To identify gray matter patterns associated with healthy aging, we first applied SSM analysis to the MRI VBM gray matter maps from the 29 healthy adult subjects in

Group 1. Focusing on the major source of variance in the gray matter maps, we initially restricted the multiple regression model to include the subject scores from the first 10 SSM component patterns. This model significantly predicted age ($F_{(10,18)}$ = 6.30, $p \leq 0.0004$) in the Group 1 cohort. A single network pattern, the first principal component, was the best and only significant individual predictor of age in the sample, accounting for 64% of the variance ($F_{(1,27)}$ = 47.11, $p < 0.000001$; **Fig. 1**). This age-related component pattern was characterized mainly by reductions in bilateral medial and dorsolateral prefrontal, perisylvian, and precuneus regions, with relative preservation in bilateral thalamus (**Fig. 2**). The locations in Talairach and Tournoux (1988) atlas coordinates for voxels with local minima and maxima pattern weights for this SSM age-related component are shown in **Table 2**. With eTIV added as an initial covariate, the age effect remained significant, accounting for 59.6% of the variance ($F_{(1,26)}$ = 45.45, $p < 0.000001$) and eTIV did not significantly contribute to the model (p = 0.19). After entering age in a separate multiple regression model, gender was not a significant predictor of the estimate of participant ages from the SSM age-related pattern (p = 0.93).

To test the reproducibility of our previously reported voxel-based SSM age-related pattern (Alexander et al., 2006), we prospectively applied the SPM2 VBM SSM pattern weights from the prior study of 26 subjects composing Group 2 to the gray matter map of each subject in Group 1. The subject expression of the previously reported age-related pattern significantly predicted age in the independent Group 1 cohort, accounting for 52% of the variance ($F_{(1,27)}$ = 28.99, $p < 0.00002$; **Fig. 3**). With eTIV added as an initial covariate, the age effect remained significant, accounting for

47% of the variance ($F_{(1,26)}$ = 26.02, p < 0.00003) and eTIV did not significantly contribute to the model (p = 0.19). After entering age in a separate multiple regression model, gender was not a significant predictor of the estimate of participant ages from the SSM age-related pattern (p = 0.57).

Because the previously reported analysis of Group 2 (Alexander et al., 2006) used SPM2 for the VBM post-processing, we performed an SSM analysis on the MRI scans from Group 2 using SPM5 VBM processing to identify network patterns of gray matter associated with age that would be directly comparable with the Group 1 SPM5 VBM SSM results. We again initially restricted the multiple regression model to include the subject scores from the first 10 SSM component patterns, and found that the model significantly predicted age ($F_{(10,15)}$ = 4.86, p < 0.004). A single network pattern, the first component, was the best and only significant predictor of age in the sample, accounting for 48% of the variance ($F_{(1,24)}$ = 22.08, p < 0.00009; **Fig. 4**). This age-related component pattern was characterized mainly by reductions in bilateral medial and dorsolateral prefrontal, superior temporal, perisylvian, and inferior parietal regions, as well as in a small area in the vicinity of the right caudate (**Fig. 5**). Regions of relative preservation in this pattern included bilateral thalamus and cerebellum. The locations in Talairach and Tournoux (1988) atlas coordinates for voxels with local minima and maxima for the age-related SSM pattern are shown in **Table 3**. With eTIV added as an initial covariate, the age effect remained significant, accounting for 48% of the variance ($F_{(1,23)}$ = 21.18, p < 0.0002) and eTIV did not significantly contribute to the model (p = 0.81). After entering age in a separate multiple regression model, gender was a significant predictor of the estimate of participant ages from the SSM age-related

pattern, accounting for an additional 11.4% of the variance over age in the model ($F_{(1,23)}$ = 6.45, $p \leq 0.018$). The men showed a higher mean expression of the age-related pattern than the women ($t(24)=2.3$, $p \leq 0.031$). This gender effect is consistent with the results previously reported for the SPM2 VBM SSM analysis of Group 2 (Alexander et al., 2006).

We subsequently combined Groups 1 and 2 into a Combined Group, 55-subject cohort and used the SSM to characterize regional covariance patterns of brain volume in relation to age. We again initially restricted the multiple regression model to include the subject scores from the first 10 SSM component patterns, and found that the model significantly predicted age ($F_{(10,44)}$ = 8.88, $p < 0.000001$). A single network pattern, the first component, was the best and only significant predictor of age in the sample, accounting for 56% of the variance ($F_{(1,53)}$ = 66.60, $p < 0.000001$; **Fig. 6**). This age-related component pattern was characterized mainly by reductions in medial and dorsolateral prefrontal, left mid temporal, right inferior temporal, supplementary motor, caudate, and to a lesser extent parietal regions, with relative preservation in the cerebellum (**Fig. 7**). The locations in Talairach and Tournoux (1988) atlas coordinates for voxels with local minima and maxima for the age-related SSM pattern are shown in **Table 4**.

Because the scans for the two groups differed in MRI scan acquisition parameters, we tested for the possibility of scan acquisition effects on our observed age-related pattern in the Combined Group cohort. Scan acquisition sequence alone was not a significant predictor of age ($p = 0.53$), and when added as an initial covariate in the multiple regression model, the age-related pattern remained unchanged,

accounting for 55% of the variance in age ($F_{(1,52)}$ = 64.78, p < 0.000001). When eTIV was added as an initial covariate (p = 0.22), the age effect also remained significant, accounting for 58% of the variance ($F_{(1,52)}$ = 76.30, p < 0.000001). After entering age in a separate multiple regression model, gender did not significantly predict the estimate of participant ages from the SSM age-related pattern (p = 0.14).

To evaluate the potential influence of APOE ε4 on the observed age-related regional gray matter pattern, we tested the association between APOE ε4 carrier status and subject expression of the age-related SSM pattern in the Combined Group cohort (n = 55). After entering age in a multiple regression model, APOE ε4 carrier status did not significantly predict the estimate of participant ages from the SSM age-related component pattern (p = 0.78).

Discussion

The results suggest that healthy aging is associated with a regionally distributed pattern of MRI gray matter reductions that has reproducible regional features, which include frontal, temporal, parietal, and subcortical brain regions. Whereas the age-related regional network patterns clearly included regions outside the frontal cortex, the frontal brain regions showed the most consistently extensive and reliable reductions across our three analysis cohorts and this was especially evident for the medial frontal cortical regions. These findings suggest that healthy human aging is associated with reproducible regional patterns of atrophy that share common regional features, including prominent reductions in frontal brain regions, but also including reductions in selective temporal, parietal, and subcortical brain areas, as part of a common

covariance network of gray matter reductions in brain aging that can vary in expression across healthy samples.

In our current study, the spatial extent of the SSM age-related pattern in Group 1 was notably greater than the pattern observed from the Combined Group. This may reflect greater variability in the Combined Group with two cohorts acquired with different scan sequences, but also suggests that the observed frontal reductions from the Combined Group analysis reflects a relatively more robust shared feature of the age-related gray matter network pattern compared to those regions showing a more diminished extent of reductions in the Combined Group. In addition, the SSM gray matter network patterns from the current study showed a greater regional extent than our previously reported age-related pattern. The analysis from the previous study (Alexander et al., 2006) used SPM2 for the VBM and did not incorporate bootstrap re-sampling. Thus, the previously reported age-related pattern used different MRI post-processing and was not adjusted on a voxel basis for variability in the regional contributions to the network pattern. Our re-analysis of the MRI scans from Group 2 using SPM5 VBM SSM with bootstrap re-sampling produced a similar regional pattern to the Group 1 result using the same analysis and post-processing methods. Although the age-related pattern from the Group 2 analysis with SPM5 SSM was highly significant with 48% of the variance explained, it was reduced compared to our Group 1 result at 64% of the variance explained and our previously reported Group 2 findings with SPM2 VBM at 66% of the variance explained, suggesting that differences between samples, post-processing methods, and scan sequences can influence the sensitivity for detecting common age-related gray matter patterns. Importantly, despite the

differences between cohorts in scan acquisition parameters, post-processing, and the possibility of age-related subject differences, common regional features of the multivariate age-related patterns were observed across all three group analyses, which may best reflect the shared regional effects of aging across the subject cohorts.

Prospective application of the prior pattern to Group 1 was highly significant, accounting for 52% of the variance and supporting the overall reproducibility of our multivariate network patterns of aging across independent samples. For each of the three analysis group cohorts, there was no difference between gender groups in chronological age. In our previous study, however, the men showed a higher expression of the age-related gray matter pattern (Alexander et al., 2006) and this gender difference was also observed in our re-analysis of the Group 2 MRI scans with SPM5 VBM SSM. The gender effect was not observed in either Group 1 or the Combined Group and may have contributed, together with scan sequence differences, to greater variability in the Combined Group analysis. Gender differences in age-related gray matter atrophy have been reported previously by some investigators (Pruessner et al., 2001), but not by others (Meyer et al., 2000). The current findings suggest that gender differences in age-related gray matter reductions can be variable across groups and may, in part, reflect a source of heterogeneity in the influence of aging on gray matter volume. It is also possible that the relatively lower variance explained in the forward application of our prior pattern to Group 1 is related to differences in scan acquisition parameters or to differences in post-processing between optimized SPM2 VBM, used in the previous study, and SPM5 VBM from the current study. We prospectively applied the pattern weights from the single network pattern that predicted age using SPM5 VBM

SSM in Group 2 to the MRI scans from Group 1; this pattern significantly predicted age in Group 1, accounting for 56% of the variance ($F_{(1,27)}$ = 34.74, $p < 0.000003$) and neither eTIV nor gender were significant predictors for Group 1.

The regional findings from our age-related pattern are generally consistent with the major findings from previous univariate analyses of regional brain volume in healthy aging (Raz et al., 1998; Good et al., 2001; Jernigan et al., 2001; Tisserand et al., 2002; Tisserand and Jolles, 2003). The differences in some regional findings between previous studies may be related to differences in the size, composition, and health status of subject samples, as well as the potential influence of genetic risk factors for neurodegenerative diseases like AD, which may be differentially represented in the respective study cohorts. Our sample was selected from a general cohort of healthy adult volunteers enrolled in a study on aging and dementia, and was rigorously screened to exclude all medical illnesses that could influence brain structure.

That APOE was not related to the age-related gray matter network in our Combined Group cohort suggests that the pattern of gray matter reductions observed in this sample cannot be explained by an increased risk for dementia due to the APOE ε4 allele. It is well established that presence of the APOE ε4 allele has been associated with reductions in cerebral metabolism in brain regions known to be preferentially affected by AD among cognitively normal, young to late middle-aged healthy adults (Reiman et al., 2004, 2005). Although our current findings, showing no association of the APOE ε4 carrier status with our age-related gray matter pattern, reduce the likelihood that the observed gray matter reductions in healthy aging reflect the very early effects of incipient dementia in this healthy cohort extending from young to elderly

adulthood, we cannot exclude the possibility of other underlying factors associated with developing disease having an influence on our gray matter pattern. It is possible that APOE ε4 may exert its greatest observable neuroimaging effects as a risk factor for late onset AD in young to late middle age. Further research is needed to evaluate the effects of APOE ε4 and other disease-related genetic risk factors on regional patterns of gray matter reduction with larger samples over the full adult age spectrum, as well as in age-specific subgroups to investigate their potential impact on the structural brain changes associated with healthy aging.

It is noteworthy that, using the same multivariate approach with VBM and bootstrap re-sampling for MRI scans acquired in young and old rhesus macaques, a pattern of frontal and selected temporal lobe gray matter reductions was observed in a non-human primate model of healthy aging in which the pathology of AD does not occur (Alexander et al., 2008). In this non-human primate study, gray matter reductions were observed in dorsolateral prefrontal regions, but not in regions of the medial frontal cortex that were prominently represented in the age-related network pattern of our human studies. Although the reductions in medial frontal regions in our human studies were consistently observed across the three group analyses, it is possible that this regional finding reflects age-associated atrophy related to widening of the anterior portion of the inter-hemispheric fissure. Further research is needed to help elucidate the implications of the differential regional effects within the frontal cortex of healthy aging found in humans and non-human primates.

Our current findings are generally consistent with those reported by Brickman et al. (2007, 2008). There are, however, some notable differences in comparison to our

studies in the approach to testing the effects of aging on brain structure. Whereas our studies included subject samples from a continuous adult age range, extending from 22 to 84 years of age, the studies by Brickman (2007, 2008) did not include middle-aged participants. Testing for regional patterns using young versus old age groups may identify patterns of group difference that may not reflect the full extent of age-related gray matter variance over the full spectrum of healthy aging. In addition, the Brickman et al. (2007, 2008) studies performed their MRI post-processing using SPM99 for the VBM procedures. Significant advances in the combined spatial normalization and tissue segmentation for VBM have since been implemented in SPM5 (Ashburner and Friston, 2005), the version used in the current study. Further, we applied bootstrap re-sampling for determining the robust regional contributions for the age-related patterns in the SSM analysis in the current study, which was not used in the previous healthy human aging studies by Brickman et al. (2007, 2008) or in our prior study (Alexander et al., 2006). By adjusting the SSM pattern weights by the variance estimates obtained from the bootstrap procedure performed over 500 iterations, we identified the regional contributions to the SSM patterns associated with healthy aging in which the potential impact of regional pattern variability related to idiosyncratic aging effects for individual subjects or subgroups within the samples are minimized (Habeck et al., 2005; Alexander et al., 2008). Thus, the age-related gray matter network patterns observed in the current study may be more likely to reflect commonly shared, robust regional features of healthy aging. Further studies are needed using larger samples to test the reproducibility of the common age-related regional pattern features observed in our study and to test the relation of patterns of gray matter atrophy with performance on

measures of cognitive abilities known to be affected in healthy aging. The development and application of a common age-related network pattern may also prove helpful in distinguishing the effects of age-related neurodegenerative disease from healthy aging. More studies are needed to evaluate the potential of such MRI multivariate gray matter patterns in aiding current efforts to help discriminate the early effects of AD from neurologically healthy aging and to potentially evaluate AD treatments effects over time. In addition, there is growing interest in studying the association of white matter changes, assessed by MRI structural and diffusion tensor imaging, as a potential factor affecting cognitive aging. Further research is needed to investigate regionally distributed patterns of white matter integrity in relation to healthy aging for comparison with our age-related gray matter patterns.

The development of methods that aid in early detection and tracking of brain changes is especially relevant to current aging research and the emerging focus on using neuroimaging techniques to evaluate treatments to delay or diminish the effects of aging, AD, or their interaction (Jack et al. 2008). This study supports the application of multivariate SSM network analysis to evaluate the regionally distributed effects of aging on the brain. SSM with MRI VBM was able to identify a robust regional pattern of gray matter that was reproducible across independent subject samples, scan sequences, and differential genetic risk for AD. With larger study cohorts, it may be possible to generate an MRI gray matter pattern representative of the effects of healthy aging that can help to detect and track age-related brain changes, as well as evaluate potential treatments or interventions designed to delay or diminish the effects of healthy and pathological aging on the brain.

Acknowledgements

The authors acknowledge grant support for this work from the NIA (AG19610, AG025526), the NIA Intramural Research Program, the Science Foundation Ireland (SFI) investigator neuroimaging program grant (08/IN.1/B1846), a translational investigator program grant by the Health Research Board (HRB) of Ireland, the Alzheimer's Association, and the state of Arizona and Arizona Department of Health Services. An early version of this work was presented, in part, at the meeting of the Society for Neuroscience, Washington, DC, November, 2008.

References

Alexander, G.E., Moeller, J.R., 1994. Application of the Scaled Subprofile Model to functional imaging in neuropsychiatric disorders: a principal component approach to modeling regional patterns of brain function in disease. Hum. Brain Mapp. 2, 79-94.

Alexander, G.E., Furey, M.L., Grady, C.L., Pietrini, P., Brady, D.R., Mentis, M.J., Schapiro, M.B., 1997. Association of premorbid intellectual function with cerebral metabolism in Alzheimer's disease: implications for the cognitive reserve hypothesis. Am. J. Psychiatry 154, 165-172.

Alexander, G.E., Mentis, M.J., Van Horn, J.D., Grady, C.L., Berman, K.F., Furey, M.L., Pietrini, P., Rapoport, S.I., Schapiro, M.B., Moeller, J.R., 1999. Individual differences in PET activation of object perception and attention systems predict face matching accuracy. NeuroReport 10, 1965-1971.

Alexander, G.E., Chen, K., Merkley, T.L., Reiman, E.M., Caselli, R.J., Aschenbrenner, M., Lewis, D.J., Pietrini, P., Teipel, S.J., Hampel, H., Rapoport, S.I., Moeller, J.R., 2006. Regional network of magnetic resonance imaging gray matter volume in healthy aging. NeuroReport 17, 951-956.

Alexander, G.E., Chen, K., Aschenbrenner, M., Merkley, T.L., Santerre-Lemmon, L.E., Shamy, J.L., Skaggs, W.E., Buonocore, M.H., Rapp, P.R., Barnes, C.A., 2008. Age-related regional network of magnetic resonance imaging gray matter in the rhesus macaque. J. Neurosci. 28, 2710-2718.

Albert, M.S., 1997. The ageing brain: normal and abnormal memory. Philos. Trans. R. Soc. Lond. B. Biol. Sci. 352:1703-1709.

Ashburner, J., Friston, K.J., 2000. Voxel-based morphometry--the methods. NeuroImage 11, 805-821.

Ashburner, J., Csernansky, J.G., Davatzikos, C., Fox, N.C., Frisoni, G.B., Thompson, P.M., 2003. Computer-assisted imaging to assess brain structure in healthy and diseased brains. Lancet Neurol. 2, 79-88.

Ashburner, J., Friston, K.J., 2005. Unified segmentation. Neuroimage 26, 839-51.

Brickman, A.M., Habeck, C., Zarahn, E., Flynn, J., Stern, Y., 2007. Structural MRI covariance patterns associated with normal aging and neuropsychological functioning. Neurobiol. Aging 28, 284-295.

Brickman, A.M., Habeck, C., Ramos, M.A., Scarmeas, N., Stern Y., 2008. A forward application of age associated gray and white matter networks. Hum. Brain Mapp. 29, 1139-1146.

Buckner, R.L., 2004. Memory and executive function in aging and AD: multiple factors that cause decline and reserve factors that compensate. Neuron 44, 195-208.

Efron, B., Tibshirani, R.J., 1994. An introduction to the bootstrap. CRC, New York.

Eidelberg, D., 1998. Functional brain networks in movement disorders. Curr. Opin. Neurol. 11, 319-326.

Eidelberg, D., Moeller, J.R., Ishikawa, T., Dhawan, V., Spetsieris, P., Chaly, T., Belakhlef, A., Mandel, F., Przedborski, S., Fahn, S., 1995a. Early differential diagnosis of Parkinson's disease with 18F-fluorodeoxyglucose and positron emission tomography. Neurology 45, 1995-2004.

Eidelberg, D., Moeller, J.R., Ishikawa, T., Dhawan, V., Spetsieris, P., Chaly, T., Robeson, W., Dahl, J.R., Margouleff, D., 1995b. Assessment of disease severity in parkinsonism with fluorine-18-fluorodeoxyglucose and PET. J. Nucl. Med. 36, 378-383.

Folstein, M.F., Folstein, S.E., McHugh, P.R., 1975. "Mini-mental state". A practical method for grading the cognitive state of patients for the clinician. J. Psychiatr. Res. 12, 189-198.

Good, C.D., Johnsrude, I.S., Ashburner, J., Henson, R.N., Friston, K.J., Frackowiak, R.S., 2001. A voxel-based morphometric study of ageing in 465 normal adult human brains. NeuroImage 14, 21-36.

Grady, C.L., Craik, F.I., 2000. Changes in memory processing with age. Curr. Opin. Neurobiol. 10, 224-231.

Habeck, C., Hilton, H.J., Zarahn, E., Flynn, J., Moeller, J., Stern, Y., 2003. Relation of cognitive reserve and task performance to expression of regional covariance net-

works in an event-related fMRI study of nonverbal memory. NeuroImage 20, 1723-1733.

Habeck, C., Krakauer, J.W., Ghez, C., Sackeim, H.A., Eidelberg, D., Stern, Y., Moeller, J.R., 2005. A new approach to spatial covariance modeling of functional brain imaging data: ordinal trend analysis. Neural Comput. 17, 1602-45.

Habeck, C., Rakitin, B.C., Moeller, J., Scarmeas, N., Zarahn, E., Brown, T., Stern, Y., 2004. An event-related fMRI study of the neurobehavioral impact of sleep deprivation on performance of a delayed-match-to-sample task. Brain Res. Cogn. Brain Res. 18, 306-321.

Jack, C.R. Jr, Bernstein, M.A., Fox, N.C., Thompson, P., Alexander, G., Harvey, D., Borowski, B., Britson, P.J., Whitwell, J., Ward, C., Dale, A.M., Felmlee, J.P., Gunter, J.L., Hill, D.L., Killiany, R., Schuff, N., Fox-Bosetti, S., Lin, C., Studholme, C., DeCarli, C.S., Krueger, G., Ward, H.A., Metzger, G.J., Scott, K.T., Mallozzi, R., Blezek, D., Levy, J., Debbins, J.P., Fleisher, A.S., Albert, M., Green, R., Bartzokis, G., Glover, G., Mugler, J., Weiner, M.W., 2008. The Alzheimer's Disease Neuroimaging Initiative (ADNI): MRI methods. J Magn Reson Imaging. 27, 685-91.

Jernigan, T.L., Archibald, S.L., Fennema-Notestine, C., Gamst, A.C., Stout, J.C., Bonner, J., Hesselink, J.R., 2001. Effects of age on tissues and regions of the cerebrum and cerebellum. Neurobiol. Aging 22, 581-594.

Meyer, J.S., Rauch, G., Rauch, R.A., Haque, A., 2000. Risk factors for cerebral hypoperfusion, mild cognitive impairment, and dementia. Neurobiol, Aging 21, 161-169.

Moeller, J.R., Strother, S.C., Sidtis, J.J., Rottenberg, D.A., 1987. Scaled subprofile model: a statistical approach to the analysis of functional patterns in positron emission tomographic data. J. Cereb. Blood Flow Metab. 7, 649-658.

Moeller, J.R., Ishikawa, T., Dhawan, V., Spetsieris, P., Mandel, F., Alexander, G.E., Grady, C., Pietrini, P., Eidelberg, D., 1996. The metabolic topography of normal aging. J. Cereb. Blood Flow Metab. 16, 385-398.

Pruessner, J.C., Collins, D.L., Pruessner, M., Evans, A.C., 2001. Age and gender predict volume decline in the anterior and posterior hippocampus in early adulthood. J. Neurosci. 21, 194-200.

Raz, N., Gunning-Dixon, F.M., Head, D., Dupuis, J.H., Acker, J.D., 1998. Neuroanatomical correlates of cognitive aging: evidence from structural magnetic resonance imaging. Neuropsychology 12, 95-114.

Reiman, E.M., Caselli, R.J., Chen, K., Alexander, G.E., Bandy, D., Frost, J., 2001. Declining brain activity in cognitively normal apolipoprotein E epsilon 4 heterozygotes: A foundation for using positron emission tomography to efficiently test treatments to prevent Alzheimer's disease. Proc. Natl. Acad. Sci. U S A 98, 3334-3339.

Reiman, E.M., Chen, K., Alexander, G.E., Caselli, R.J., Bandy, D., Osborne, D., Saunders, A.M., Hardy, J., 2004. Functional brain abnormalities in young adults at genetic risk for late-onset Alzheimer's dementia. Proc. Natl. Acad. Sci. U S A. 101, 284-9.

Reiman, E.M., Chen, K., Alexander, G.E., Caselli, R.J., Bandy, D., Osborne, D., Saunders, A.M., Hardy, J., 2005. Correlations between apolipoprotein E epsilon4

gene dose and brain-imaging measurements of regional hypometabolism. Proc. Natl. Acad. Sci. U S A.102, 8299-302.

Rypma, B., Prabhakaran, V., Desmond, J.E., Gabrieli, J.D., 2001. Age differences in prefrontal cortical activity in working memory. Psychol. Aging16, 371-384.

Saunders, A.M., Strittmatter, W.J., Schmechel, D., George-Hyslop, P.H., Pericak-Vance, M.A., Joo, S.H., Rosi, B.L., Gusella, J.F., Crapper-MacLachlan, D.R., Alberts, M.J., Hulette, C., Crain, B., Goldgaber, D., Roses, A.D., 1993. Association of apolipoprotein E allele epsilon 4 with late-onset familial and sporadic Alzheimer's disease. Neurology 43, 1467-1472.

Smith, J.F., Chen, K., Johnson, S., Morrone-Strupinsky, J., Reiman, E.M., Nelson, A., Moeller, J.R., Alexander, G.E., 2006. Network analysis of single-subject fMRI during a finger opposition task. NeuroImage 32, 325-332.

Stern, Y., Habeck, C., Moeller, J., Scarmeas, N., Anderson, K.E., Hilton, H.J., Flynn, J., Sackeim, H., van Heertum, R., 2005. Brain networks associated with cognitive reserve in healthy young and old adults. Cereb. Cortex 15, 394-402.

Talairach, J., Tournoux, P, 1988. Co-planar Stereotaxic Atlas of the Human Brain: 3-Dimensional Proportional System - an Approach to Cerebral Imaging. Thieme Medical Publishers, New York.

Tisserand, D.J., Pruessner, J.C., Sanz Arigita, E.J., van Boxtel, M.P., Evans, A.C., Jolles, J., Uylings, H.B., 2002. Regional frontal cortical volumes decrease differentially in aging: an MRI study to compare volumetric approaches and voxel-based morphometry. NeuroImage 17, 657-669.

Tisserand, D.J., Jolles, J., 2003. On the involvement of prefrontal networks in cognitive ageing. Cortex 39, 1107-1128.

Van Petten, C., Plante, E., Davidson, P.S., Kuo, T.Y., Bajuscak, L., Glisky, E.L., 2004. Memory and executive function in older adults: relationships with temporal and prefrontal gray matter volumes and white matter hyperintensities. Neuropsychologia 42, 1313-1335.

West, R.L., 1996. An application of prefrontal cortex function theory to cognitive aging. Psychol. Bull. 120, 272-292.

Figure Legends

Figure 1. Regression of subject scores from the SSM network analysis of MRI SPM5 VBM predicting age in 29 healthy adults (Group 1), 22-84 years of age. Predicted age is derived from the subject scores for the first SSM component pattern.

Figure 2. Projection map of MRI gray matter reflecting the first SSM component pattern whose subject scores predicted age in 29 healthy adults (Group 1). The blue end of the color scale indicates areas of decreased gray matter volume with increasing age, whereas the orange end of the color scale indicates areas of relatively increased gray matter (i.e., preservation) with increasing age. Subjects with high positive scores for this age-related pattern have relatively greater reductions in blue areas and relatively greater covarying increases in orange areas. Only voxels with Z scores ≥ +2 and ≤ -2, after bootstrap re-sampling to provide robust regional pattern weights, are shown.

Figure 3. Regression of subject scores from the prospective application of a previously identified SPM2 VBM SSM network pattern predicting age in an independent sample of 29 healthy adults (Group 1), 22-84 years of age. Predicted age is derived from the subject scores for the prospectively applied pattern that reflects a linear combination of the first three SSM component patterns associated with age in the previously reported sample of 26 subjects (Group 2; Alexander et al., 2006).

Figure 4. Regression of subject scores from the SSM network analysis of MRI SPM5 VBM predicting age in 26 healthy adults (Group 2), 22-77 years of age. Predicted age is derived from the subject scores for the first SSM component pattern.

Figure 5. Projection map of MRI gray matter reflecting the first SSM component pattern whose subject scores predicted age in 26 healthy adults (Group 2). The blue end of the color scale indicates areas of decreased gray matter volume with increasing age, whereas the orange end of the color scale indicates areas of relative increased gray matter with increasing age. Subjects with high positive scores for this age-related pattern have relatively greater reductions in blue areas and relatively greater covarying increases in orange areas. Only voxels with Z scores ≥ +2 and ≤ -2, after bootstrap re-sampling to provide robust regional pattern weights, are shown.

Figure 6. Regression of subject scores from the SSM network analysis of MRI SPM5 VBM predicting age in 55 healthy adults (Combined Group), 22-84 years of age. Predicted age is derived from the subject scores for the first SSM component pattern.

Figure 7. Projection map of MRI gray matter reflecting the first SSM component pattern whose subject scores predicted age in 55 healthy adults (Combined Group). The blue end of the color scale indicates areas of decreased gray matter volume with increasing age, whereas the orange end of the color scale indicates areas of relative increased gray matter with increasing age. Subjects with high positive scores for this age-related pattern have relatively greater reductions in blue areas and relatively greater covarying

increases in orange areas. Only voxels with Z scores ≥ +2 and ≤ -2, after bootstrap re-sampling to provide robust regional pattern weights, are shown.

Table 1. Subject characteristics

	Group 1	Group 2	Combined Group
N	29	26	55
Age (mean ± sd)	47.7±18.7	50.7±15.6	49.1±17.2
Gender (M / F)	11 / 18	15 / 11	26 / 29
MMSE (mean ± sd)	29.7±0.5	29.6±0.7	29.7±0.5
APOE status (ε4 carriers / noncarriers)	9 / 20	10 / 16	19 / 36

sd, standard deviation; M, male; F, female; MMSE, Mini-Mental State Exam; APOE, apolipoprotein E.

Table 2. Location of regions in SSM age-related network pattern in Group 1 (n = 29)

Region	H	BA	Talairach coord.			Z
			x	y	z	
Minima						
Inf frontal	R	44	55	18	25	3.70
	R	47	47	16	-8	3.60
	L		-50	22	-4	2.84
Mid frontal	R	9	38	41	31	3.98
	L	46	-47	36	24	2.87
Sup frontal	R	8	22	38	42	3.33
	L	8	-25	41	38	3.34
Sup med frontal		8	2	27	39	4.48
		8	0	44	42	4.25
		9	1	43	27	4.24
		10	0	53	1	3.34
		6	0	5	48	3.41
Anterior cingulate		32	1	19	40	3.97
		32	-1	50	9	2.86
Paracentral		7	0	-32	53	2.73
Precuneus	R	7	12	-76	44	3.79

Table 2,cont. Location of regions in SSM age-related network pattern in Group 1 (n = 29)

	L	7	-4	-70	48	2.63
Insula/Perisylvian	R		42	-5	0	4.06
	R		41	12	-11	3.51
	L		-43	-4	0	3.32
	L		-50	11	-4	3.01
Pre/Postcentral	R	4	54	-7	45	3.01
	R	2	45	-25	57	2.68
	L	40	-56	-22	45	3.08

Inf parietal	R	40	46	-48	50	2.44
Sup temporal	R	22	64	-47	17	2.78
	R	22	62	2	4	3.22
	L	22	-61	0	0	2.71
	L	22	-63	-53	17	3.05
Fusiform	R	37	51	-48	-21	3.35
	L	37	-50	-68	-13	2.03
Caudate	R		7	16	3	3.63
	L		-10	13	10	3.66
Cerebellum	R		47	-43	-25	3.41

Table 2,cont. Location of regions in SSM age-related network pattern in Group 1 (n = 29)

Maxima						
Inf frontal	L	47	-42	38	-12	2.62
Mid frontal	L	10	-34	46	-6	2.86
Middle cingulate	R	24	8	-4	33	2.26
	L	23	-7	-12	34	2.56
Posterior cingulate	R	23	10	-45	24	2.55
	L	30	-10	-48	21	2.22
Inf temporal	L	20	-35	-5	-30	3.21
Temporal pole	R	38	41	9	-24	2.50
	L	21	-37	6	-27	2.56
Lingual	R	18	16	-74	4	2.97
	L	18	-14	-79	4	2.80
Thalamus	R		17	-25	5	2.46
	L		-13	-21	5	2.41
Putamen	R		28	9	-4	2.76
	L		-26	15	-1	2.75
Cerebellum	R		15	-70	-23	3.21
	R		16	-71	-27	2.88

	L	-6	-63	-20	2.42

Table 2,cont. Location of regions in SSM age-related network pattern in Group 1 (n = 29)

Location of regions in SSM age-related network pattern, 29 subjects. SSM, Scaled Subprofile Model; H, hemisphere; BA, Brodmann area; Talairach coord, Talairach and Tournoux anatomical atlas coordinates in x, y, and z planes; Z, Z score; Minima, local minima for negative SSM pattern weights for regions with Z scores ≤ -2; Maxima, local maxima for positive SSM pattern weights for regions with Z scores ≥ +2; Inf frontal, inferior frontal region; Mid frontal, middle frontal region; Sup frontal, superior frontal region; Sup med frontal, superior medial frontal region; Paracentral, paracentral region; Insula/Perisylvian, regions of the insula and perisylvian fissure; Pre/Postcentral, pre- and post-central regions; Inf parietal, inferior parietal region; Sup temporal, superior temporal region; Fusiform, region of the fusiform gyrus; Inf temporal, inferior temporal region; Lingual, region of the lingual gyrus.

Table 3. Location of regions in SSM age-related network pattern in Group 2 (n = 26)

Region	H	BA	Talairach coord.			Z
			x	y	z	
Minima						
Inf frontal	R	44	53	19	21	3.40
	L	45	-48	17	29	3.40
Mid frontal	R	46	28	53	27	3.00
	L	10	-31	53	19	3.19
Sup frontal	R	10	21	65	-10	2.59
	L	9	-26	45	35	2.26
Sup med frontal		9	3	52	31	2.61
		10	1	58	19	2.84
		9	-2	45	16	2.75
		6	-2	8	51	2.94
Anterior cingulate	32		4	5	44	3.44
	24		0	-2	44	2.91
Posterior cingulate	31		0	-24	42	2.46
Paracentral		5	-1	-25	45	2.94
Cuneus	R	18	3	-88	27	2.52
Insula/Perisylvian	R		45	16	-8	2.86

Table 3, cont. Location of regions in SSM age-related network pattern in Group 2 (n = 26)

	L		-43	16	-1	2.45
Pre/Postcentral	R	4	49	-8	52	2.53
	R	1	57	-15	45	3.02
	L	6	-57	-7	37	2.41
Inf parietal	R	40	46	-37	50	2.79
	L	40	-46	-35	46	3.51
	L	40	-63	-48	25	2.84
Mid temporal	R	39	50	-73	18	2.16

	L	39	-56	-58	14	2.02
Sup temporal	R	22	68	-25	1	2.46
	L	22	-64	-47	21	2.81
	L	22	-58	-54	17	2.45
Fusiform	L	37	-52	-57	-17	2.84
Mid occipital	R	19	33	-71	40	2.52
Sup occipital	R	7	33	-69	44	2.47
Calcarine		17	2	-93	5	2.30
Caudate	R		9	21	3	2.14
Maxima						
Inf / orbital frontal	R	47	20	17	-14	2.32

Table 3, cont. Location of regions in SSM age-related network pattern in Group 2 (n = 26)

	L	47	-17	18	-14	3.33
Sup med frontal	L	10	-14	58	-3	2.11
Inf temporal	R	20	44	-5	-27	2.40
	L	20	-43	-6	-27	3.18
Mid temporal	R	21	56	-10	-16	2.73
	L	21	-46	3	-27	2.85
Temporal pole	R	21	37	0	-27	2.58
	L	20	-32	-4	-30	2.94
Thalamus	R		10	-18	5	2.93
	L		-9	-20	5	2.56
Cerebellum	R		13	-72	-27	3.09
	L		-39	-56	-27	2.93

Table 3, cont. Location of regions in SSM age-related network pattern in Group 2 (n = 26)

Location of regions in SSM age-related network pattern, 26 subjects. SSM, Scaled Subprofile Model; H, hemisphere; BA, Brodmann area; Talairach coord, Talairach and Tournoux anatomical atlas coordinates in x, y, and z planes; Z, Z score; Minima, local minima for negative SSM pattern weights for regions with Z scores ≤ -2; Maxima, local maxima for positive SSM pattern weights for regions with Z scores ≥ +2; Inf frontal, inferior frontal region; Mid frontal, middle frontal region; Sup frontal, superior frontal region; Sup med frontal, superior medial frontal region; Paracentral, paracentral region; Insula/Perisylvian, regions of the insula and perisylvian fissure; Pre/Postcentral, pre- and post-central regions; Inf parietal, inferior parietal region; Mid temporal, middle temporal region; Sup temporal, superior temporal region; Fusiform, region of the fusiform gyrus; Mid occipital, middle occipital region; Sup occipital, superior occipital region; Inf/orbital frontal, region of the inferior and orbital frontal gyri; Inf temporal, inferior temporal region.

Table 4. Location of regions in SSM age-related network pattern in the Combined Group (n = 55)

Region	H	BA	Talairach coord			Z
			x	y	z	
Minima						
Inf frontal	R	45	56	18	21	2.26
	R	44	50	18	32	2.31
Mid frontal	R	9	33	43	35	2.12
	L	9	-25	44	35	2.37
Sup frontal	R	8	24	38	42	2.26
	L	8	-25	41	38	2.52
Sup med frontal		6	2	8	44	3.29
		8	1	33	50	2.56
		8	0	44	38	2.73
		8	-1	44	20	2.78
Anterior cingulate		32	-1	11	40	2.89
		32	-2	45	12	2.38
Paracentral		5	0	-25	45	2.47
Inf parietal	L	40	-55	-24	45	2.37

Table 4, cont. Location of regions in SSM age-related network pattern in the Combined Group (n = 55)

	L	40	-41	-50	50	2.07
	R	40	62	-48	25	2.08
Insula/Perisylvian	R		45	15	-7	2.77
	R		42	12	-11	2.74
	L		-42	-4	4	2.16
Mid temporal	R	21	68	-26	1	2.17
Sup temporal	L	21	-60	-53	21	2.18
Fusiform	R	20	50	-49	-21	2.56
Caudate	R		10	14	10	2.59
	L		-9	12	10	2.69

Maxima						
Thalamus	R		19	-27	5	2.21
Cerebellum	R		16	-71	-23	2.68
	L		-39	-57	-27	2.02
Inf temporal	L	20	-34	-5	-30	2.49
Temporal pole	R		32	4	-27	2.27
	L		-37	6	-27	2.40

Table 4, cont. Location of regions in SSM age-related network pattern in the Combined Group (n = 55)

Location of regions in SSM age-related network pattern, 55 subjects. SSM, Scaled Subprofile Model; H, hemisphere; BA, Brodmann area; Talairach coord, Talairach and Tournoux anatomical atlas coordinates in x, y, and z planes; Z, Z score; Minima, local minima for negative SSM pattern weights for regions with Z scores ≤ -2; Maxima, local maxima for positive SSM pattern weights for regions with Z scores ≥ +2; Inf frontal, inferior frontal region; Mid frontal, middle frontal region; Sup frontal, superior frontal region; Sup med frontal, superior medial frontal region; Paracentral, paracentral region; Inf parietal, inferior parietal; Insula/Perisylvian, regions of the insula and perisylvian fissure; Mid temporal, middle temporal region; Sup temporal, superior temporal region; Fusiform, region of the fusiform gyrus; Inf temporal, inferior temporal region.

Figure 1.

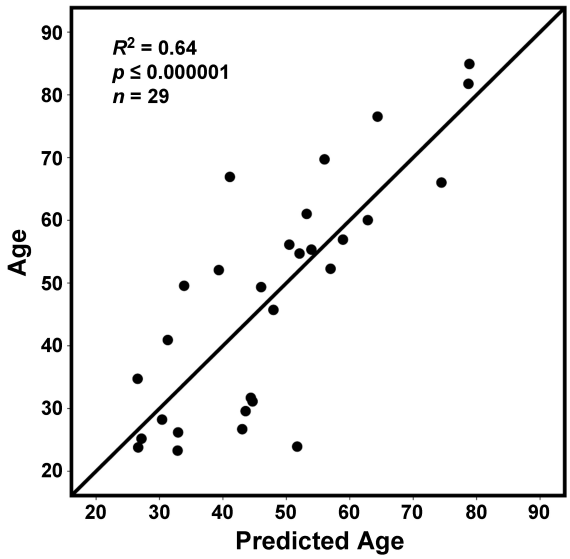

Figure 2.

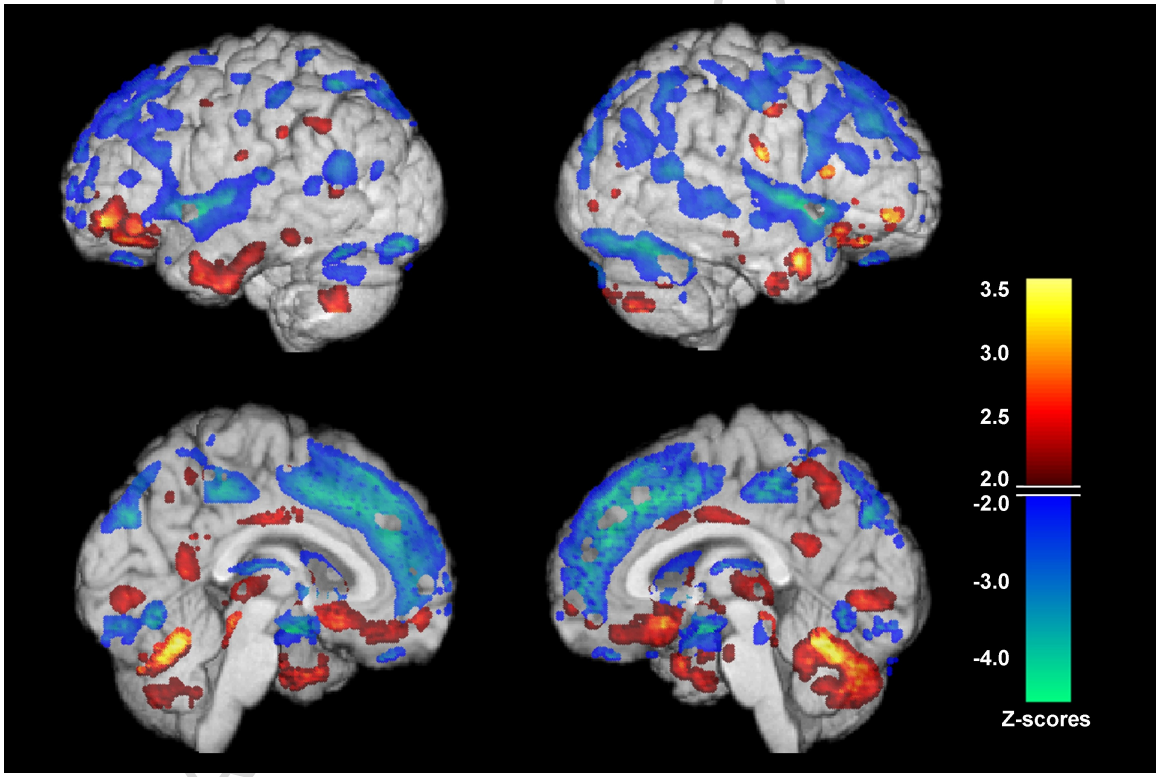

Figure 3.

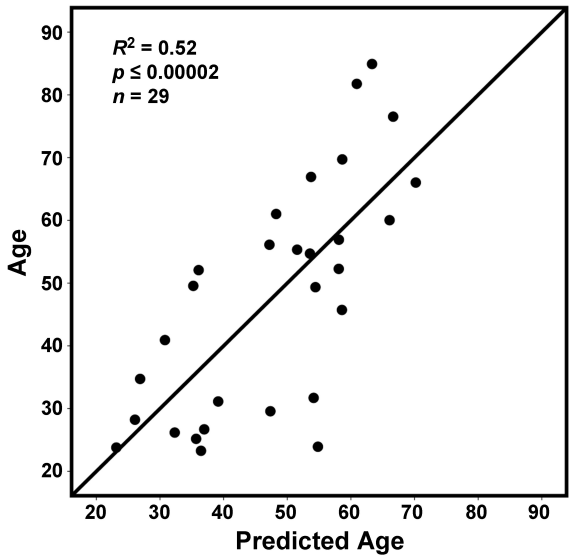

Figure 4.

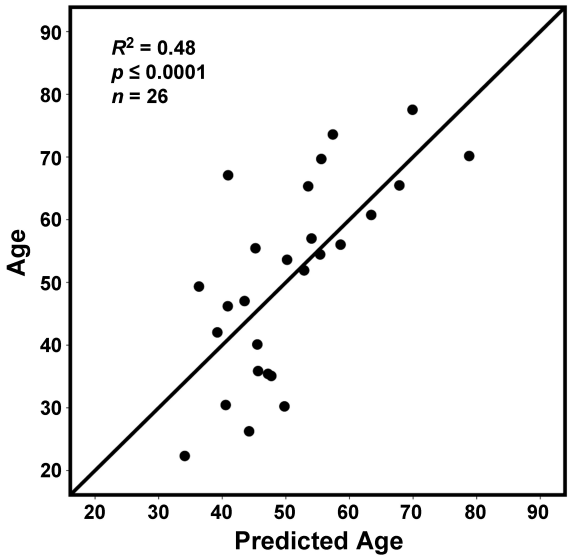

Figure 5.

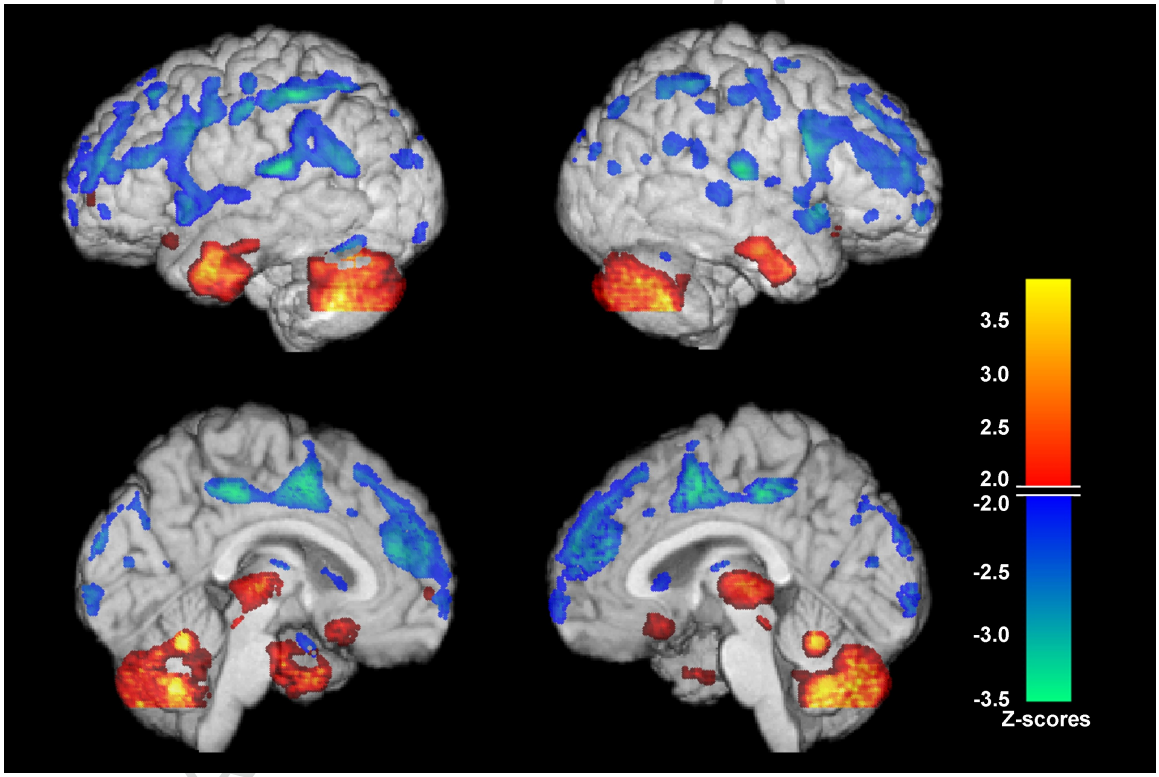

Figure 6.

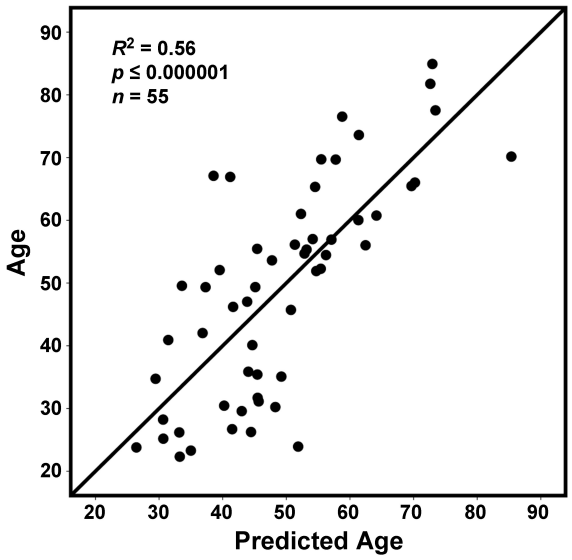

Figure 7.